19th International Conference
ENGINEERING MECHANICS 2013
Svratka, Czech Republic, May 13 – 16, 2013

PARALLEL NUMERICAL SIMULATION OF AIRFLOW PAST AN OSCILLATING NACA0015 AIRFOIL

V. Řidký[*], P. Šidlof[**] and V. Vlček[***]

Abstract: *This paper focuses on 3D and 2D parallel computation of pressure and velocity fields around an elastically supported airfoil self-oscillating due to interaction with the airflow The results of numerical simulations are compared with data measured in a wind tunnel, where physical model of a NACA0015 airfoil was mounted and tuned to exhibit the flutter instability. The experimental results were obtained previously in the Institute of Thermomechanics by interferometric measurements in a subsonic wind tunnel in Nový Knín. For the numerical solution is implemented in OpenFOAM, an open-source software package based on finite volume method. In the numerical solution is prescribed displacement of the airfoil, which corresponds to the experiment.*

Keywords: ***Airfoil, CFD, parallel computing, OpenFOAM.***

1. Introduction

The interaction of fluids and elastic structures is very important in engineering field. The fluid-structure interactions can be found e.g. in applications such as aerospace engineering, turbine design or biomechanics. The interaction between fluids and vibrating structures is the main subject of aeroelasticity.

The classical methods of aeroelasticity are usually based on a simplified flow model (e.g. Bernoulli or Euler equations) coupled with a lumped-parameter structural model [Dowel 1978]. In more complex flow regimes, e. g. stall flutter of airfoils with massive flow separation, we cannot use this simplified approach, and the airflow has to be modeled by Navier-Stokes equations. Turbulent flow has a three-dimensional character and so 3D simulations are preferable, but in a number of cases, two-dimensional models are still applied from practical reasons (mainly because the computational cost is drastically lower).

For the numerical solution of turbulent flow, three basic approaches are possible. First approach is direct numerical simulations (DNS), where the Navier-Stokes equations are discretized and solved directly and all turbulent scales are resolved. Second method is Large Eddy Simulations (LES), where large coherent turbulent structures are resolved and the small-scale isotropic turbulence is modeled by means of a sub-grid scale model. The most frequently used approach is the Reynolds-averaged Navier-Stokes (RANS), where the Reynolds stresses can be modeled by a vast variety of turbulence models. However, in many technical applications, especially when the airflow is separated, RANS models give incorrect results.

The current paper is focused on a parallel numerical solution of incompressible airflow past a NACA0015 airfoil using 2D and 3D computational meshes, and comparison of the numerical results with experimental data measured in aerodynamic tunnel of the Institute of Thermomechanics in Nový Knín. Specifically, the simulated distribution of pressure on the surface of the wing vibrating in the channel due to flutter instability is compared to the experimental surface pressures. In the experiment,

[*] Ing. Václav Řidký: Institute of Thermomechanics AS CR, v. v. i., Dolejškova 1402/5; 182 00, Praha 8; CZ, e-mail: vaclav.ridky@tul.cz

[**] Ing. Petr Šidlof, Ph.D.: Institute of Thermomechanics AS CR, v. v. i., Dolejškova 1402/5; 182 00, Praha 8; CZ, e-mail: sidlof@it.cas.cz

[***] Ing. Václav Vlček, Csc.: Institute of Thermomechanics AS CR, v. v. i., Dolejškova 1402/5; 182 00, Praha 8; CZ, e-mail: vlcek@it.cas.cz

the pressures are evaluated from interferograms obtained using Mach-Zehnder interferograms, as described in [Vlček 2010].

2. Methods

2.1. Mathematical model, geometry, mesh and boundary conditions

Geometry of the computational domain corresponds to experimental setup, where the airfoil is placed in a channel with a cross-section of 210 x 80 mm. The length of the computational domain is set to 580 mm (see Fig. 1). The shape of NACA0015 airfoil is described by the equation

$$y = \frac{t}{0.2} c \left[0.2969 \sqrt{\frac{x}{c}} - 0.1260 \left(\frac{x}{c}\right) - 0.3516 \left(\frac{x}{c}\right)^2 + \; -0.1015 \left(\frac{x}{c}\right)^4 \; 0.2843 \left(\frac{x}{c}\right)^3 \right], \qquad (1)$$

where $t = 15$ is the ratio of the greatest profile thickness to chord length, $c = 65{,}5\ mm$ is the chord length, x is the position of a point on the profile along the chord running from 0 to c, y is half the thickness of the profile for a given value of x.

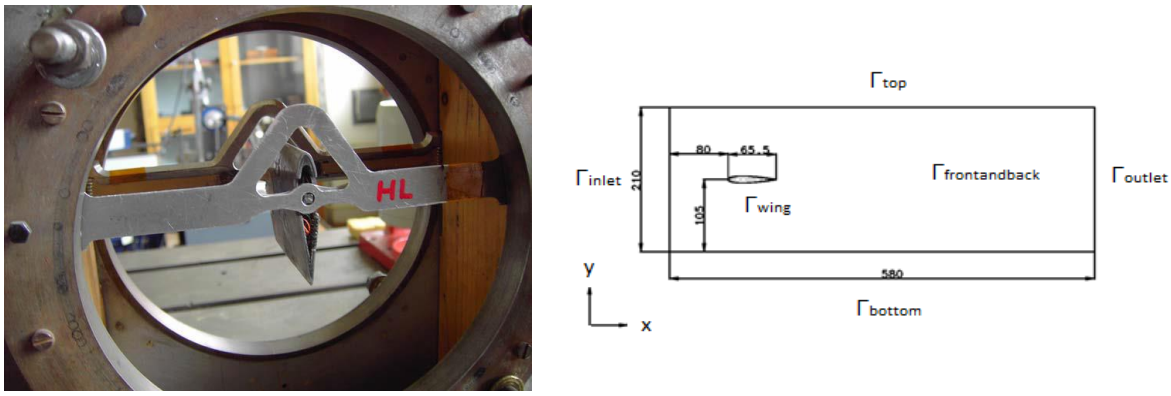

Fig. 1: Measurement setup [Kozánek 2010] and computational domain with boundaries

On the geometry was generated 3D and 2D mesh. The 3D mesh consists of 895000 mostly hexahedral elements, the 2D mesh consists of 139000 quadrangular elements. Both meshes are deformed during the numerical solution due to the oscillation of the wing. The position of the mesh nodes is computed from the mesh velocity $\boldsymbol{w}$, which is calculated from the Laplace equation with spatially variable diffusivity γ:

$$\nabla \cdot (\gamma \nabla \boldsymbol{w}) = 0 \qquad (2)$$

The boundary conditions for the auxiliary problem are as follows: the mesh velocity $\boldsymbol{w}$ is zero on the fixed boundaries, and equal to the airfoil velocity on the airfoil surface.

The flow pas the moving airfoil is described by incompressible Navier-Stokes equations

$$\nabla \cdot \boldsymbol{u} = 0 \qquad (3)$$

$$\frac{\partial \boldsymbol{u}}{\partial t} + \nabla \cdot (\boldsymbol{u}\boldsymbol{u}) - \nabla \cdot \nu \Delta \boldsymbol{u} + \frac{1}{\rho} \nabla p = 0\,, \qquad (4)$$

where $\boldsymbol{u}$ is flow velocity, p is dynamic pressure, ν is kinematic viscosity and ρ is density. These equations are in strong conservative form, suitable for finite volume discretization.

Boundary conditions for the pressure and velocity fields are specified as follows: on fixed walls, the flow velocity $\boldsymbol{u}$ is zero, on the moving wing surface the flow velocity is equal to the velocity of the airfoil. At the inlet Γ_{inlet} a flat velocity profile u_x = 147 m/s is prescribed. At the outlet Γ_{out}, the pressure is set to zero. Due to large intensity of vorticity resulting from flow separation downstream of the wing, a stabilized boundary condition for the velocity is prescribed at Γ_{out}: $\partial \boldsymbol{u}/\partial n = 0$ when velocity direction points outward of the domain, u_x = 0 m / s otherwise, for pressure p = 0 Pa.

3. Results

During the experiment, the airfoil was placed on elastic support allowing vibration with two degrees of freedom: pitch (rotation about the elastic axis, located in 1/3 of the chord length) and plunge (vertical motion). The flow fields were measured by Mach-Zehnder interferometer and high-speed camera (more details can be found in [Vlček 2010 and Vlček 2011]). The amplitude of the rotational movement was ± 17 °, and the amplitude of the plunging movement was ± 7 mm. The motion of the airfoil in the numerical simulation was prescribed according to vibratory patterns identified from the experiment [Vlček 2011]. The frequency of vibration of the airfoil was 19,5 Hz.

Simulated pressure fields on the airfoil surface, averaged over five periods of vibration, are compared with experimental data in Figs. 2-8. The figures in the left show the normalized pressure field around the airfoil in seven specific phases of one vibration period T = 51,3 ms. The phases, where the data evaluated from the experiment are available, are denoted by indices 002, 004, 006 .. 014. The reference pressure p_0 is taken as the pressure at inlet. The zero pitch of the airfoil occurs near phase 013, the time interval between the phases is 2 ms. The graphs on the right shows the normalized pressure distribution along the bottom surface of the airfoil, and compare the 2D and 3D numerical simulation with the experimental data.

The values of p/p_0 in the range 1,02 up to 1,04, found in the numerical simulations near the stagnation point, are physically incorrect. This is probably caused by minor inconsistency between the model and the experiment, mainly by the simplified velocity boundary condition at the inlet, which inevitably differs from the real inflow conditions.

On the top surface of the airfoil where massive flow separation occurs, the numerical results and experimental data differ significantly (the results are not shown here). This is mainly because the current numerical simulation is run without turbulence model and with insufficiently fine mesh in the boundary layer. Numerical modeling of the separated boundary layer is actually a very challenging and problematic issue, and even sophisticated turbulence models used in advanced RANS simulations do not give reliable results in many cases.

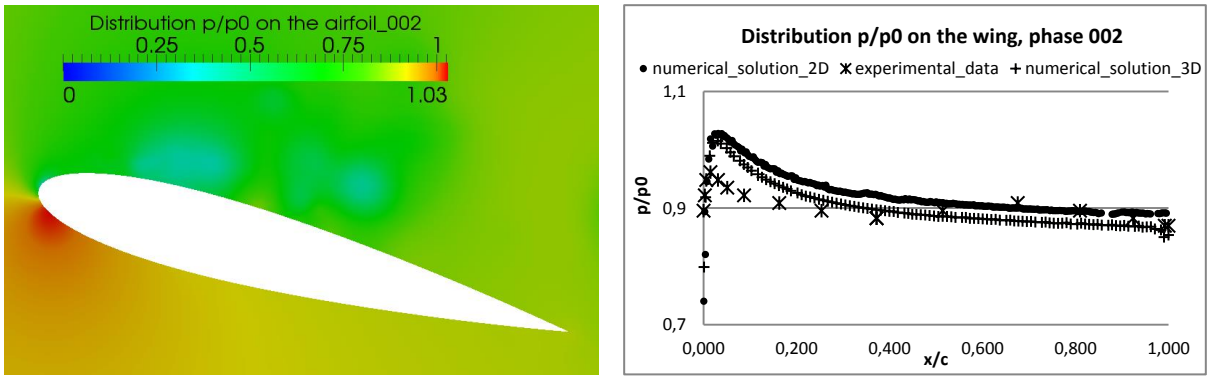

Fig. 2: Normalized pressure field from the numerical simulation (left), normalized pressure distribution p/p_0 on the bottom surface from experiment, 2D and 3D simulation (right), phase 002.

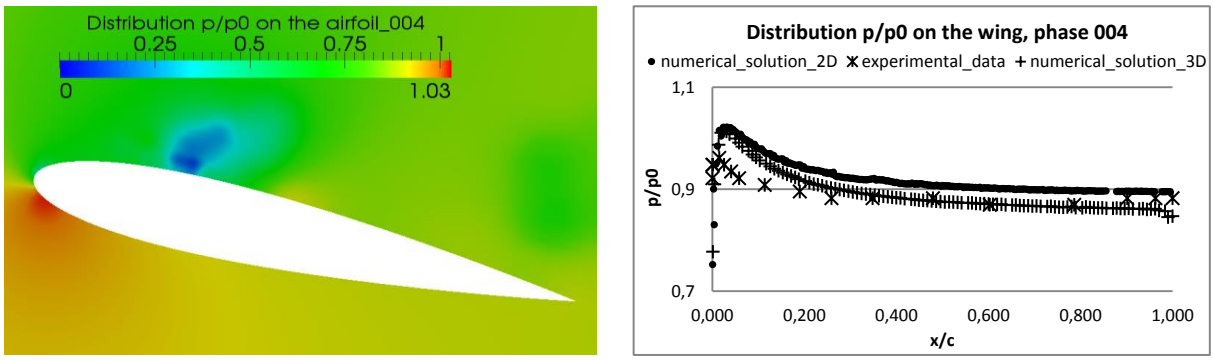

Fig. 3: Normalized pressure field from the numerical simulation (left), normalized pressure distribution p/p_0 on the bottom surface from experiment, 2D and 3D simulation (right), phase 004.

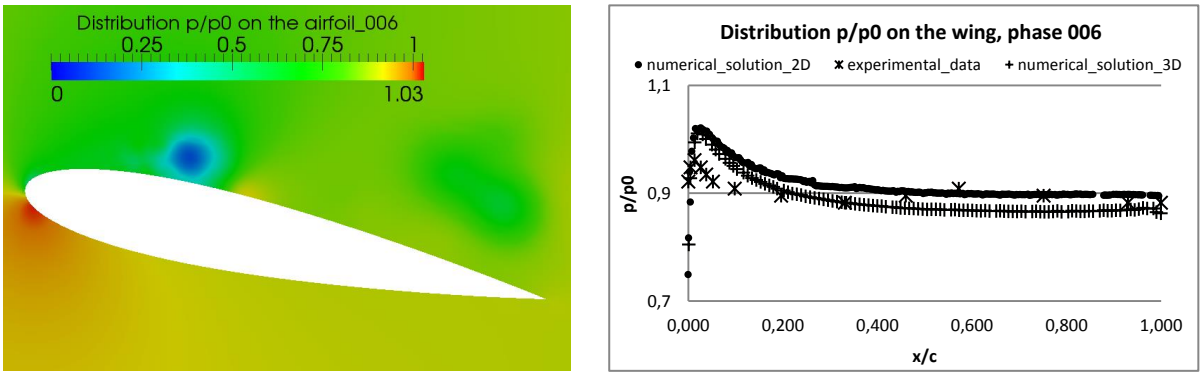

Fig. 4: Normalized pressure field from the numerical simulation (left), normalized pressure distribution p/p_0 on the bottom surface from experiment, 2D and 3D simulation (right), phase 006.

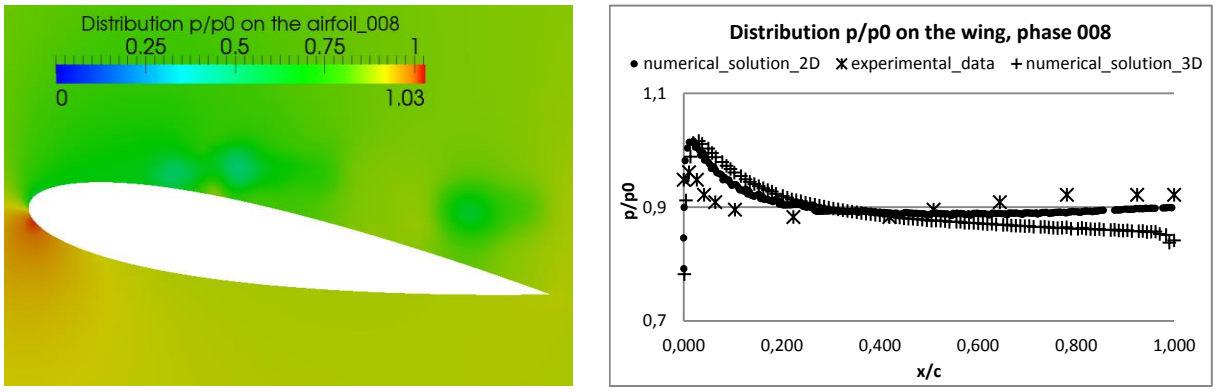

Fig. 5: Normalized pressure field from the numerical simulation (left), normalized pressure distribution p/p_0 on the bottom surface from experiment, 2D and 3D simulation (right), phase 008.

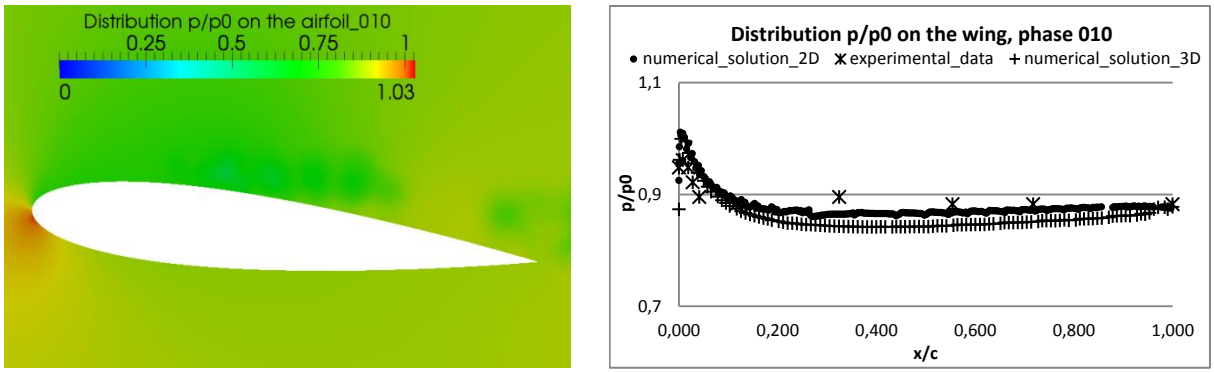

Fig. 6: Normalized pressure field from the numerical simulation (left), normalized pressure distribution p/p_0 on the bottom surface from experiment, 2D and 3D simulation (right), phase 0010.

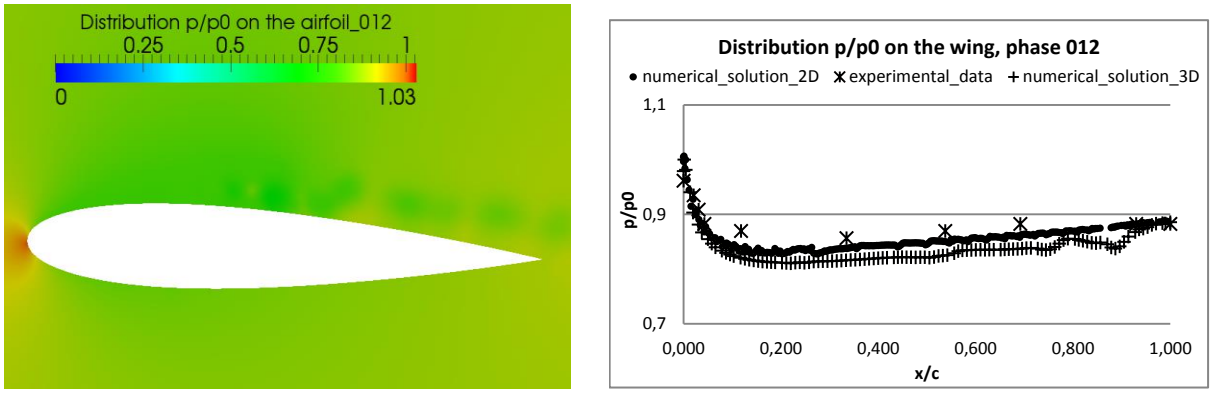

Fig. 7: Normalized pressure field from the numerical simulation (left), normalized pressure distribution p/p_0 on the bottom surface from experiment, 2D and 3D simulation (right), phase 012.

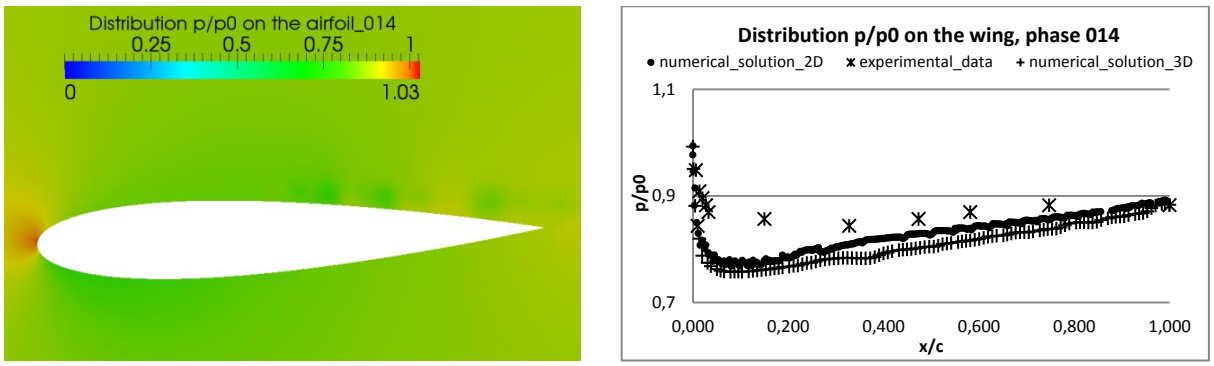

Fig. 8: Normalized pressure field from the numerical simulation (left), normalized pressure distribution p/p_0 on the bottom surface from experiment, 2D and 3D simulation (right), phase 014.

4. Conclusions

3D and 2D numerical simulations of airflow past a vibrating airfoil were performed and compared with experimental data. The large meshes required in 3D CFD simulations need to be parallelized in order to achieve reasonable computation times. The current numerical model provides good match with the experimental data only in the regions, where there is no flow separation. In the separated regions, the results of numerical simulation and experiments are very different. This is probably caused by the fact that for the purpose of this preliminary study, a simple incompressible model without any turbulence modelling was chosen. The evaluation of the interferographic images, on the other hand, is also problematic, especially in the regions of high density gradients. In the future, it will be appropriate to switch to the compressible flow model and possibly incorporate a suitable turbulence model.

Acknowledgement

The research has been supported by the Czech Science Foundation, project P101/11/0207

References

Dowel, E. (1978) *A modern course in aeroelasticity*. Sijthoff & Noordhoff International Publishers B. V., Alphen aan den Rijn.

Feistauer M., Horáček J., Růžička M., Sváček P. (2011) *Numerical analysis of flow induced nonlinear vibrations of an airfoil with three degrese of freedom*. Computers & Fluids, **49**, pp. 110-127.

Kozánek J., Bula V., Zolotarev I. (2010) *Matematický model uložení zkušebního aerodynamického profilu* Seminář Interakce a zpětné vazby 2010.

Vlček V., Kozánek J. (2010) *Preliminary interferometry measurements of flow field around a fluttering NACA0015 profile*. Engineering Mechanics 2010, pp. 540–550.

Vlček V., Kozánek J., Zolotarev I. (2011) *Forces acting on the fluttering profile in the wind tunnel*. Vibration problems ICOVP 2011 - Supplement, 2011, pp. 516–522.

The OpenFOAM foundation. OpenFOAM User Guide;2013 http://www.openfoam.org/docs/user/